Study of Air Bubble Induced Light Scattering Effect On Image Quality in 193 nm Immersion Lithography

Yongfa Fan, Neal Lafferty, Anatoly Bourov, Lena Zavyalova, Bruce W. Smith
Rochester Institute of Technology, Microelectronic Engineering Department
82 Lomb Memorial Drive, Rochester, NY 14623

ABSTRACT

As an emerging technique, immersion lithography offers the capability of reducing critical dimensions by increasing numerical aperture (NA) due to the higher refractive indices of immersion liquids than that of air. Among the candidates for immersion liquids, water appears to be an excellent choice due to its high transparency at a wavelength of 193 nm, as well as its immediate availability and low processing cost. However, in the process of forming a water fluid layer between the resist and lens surfaces, air bubbles are often created due to the high surface tension of water. The presence of air bubbles in the immersion layer will degrade the image quality because of the inhomogeneity induced light scattering in the optical path. Therefore, it is essential to understand the air bubble induced light scattering effect on image quality. Analysis by geometrical optics indicates that the total reflection of light causes the enhancement of scattering in the region where the scattering angle is less than the critical scattering angle, which is 92 degrees at 193 nm. Based on Mie theory, numerical evaluation of scattering due to air bubbles, polystyrene spheres and PMMA spheres was conducted for TE, TM or unpolarized incident light. Comparison of the scattering patterns shows that the polystyrene spheres and air bubbles resemble each other with respect to scattering properties. Hence polystyrene spheres are used to mimic air bubbles in studies of lithographic imaging of "bubbles" in immersion water. In direct interference lithography, it is found that polystyrene spheres (2 μm in diameter) 0.3 mm away from the resist surface would not image, while for interferometric lithography at 0.5NA, this distance is estimated to be 1.3 mm. Surprisingly, polystyrene spheres in diameter of 0.5 μm (which is 5 times larger than the interferometric line-width) will not image. It is proposed that "bubbles" are repelled from contact with the resist film by surface tension. The scatter of exposure light can be characterized as "flare". This work shows that microbubbles are not a technical barrier to immersion lithography.

Keywords: Optical lithography, immersion, Mie scattering

1. INTRODUCTION

Driven by the demands in the microelectronic industry to produce smaller device geometries, conventional optical lithography has extended critical dimensions down to 65 nm using a 193 nm ArF excimer laser, along with the employment of resolution enhancement techniques such as high NA, phase-shift masking, off-axis illumination, optical proximity correction, pupil filtering, etc. It seems that the solution for the 45-65 nm technology node is to resort to a shorter wavelength illumination source, as was true in the past lithography generations. Unfortunately, at the wavelength of 157 nm, the inherent properties of DUV light has generated virtually insurmountable barriers to lithographic practice, especially in the aspects of imaging and masking materials. In the past few years, the difficulties in tackling these barriers have turned attentions to another alternative: immersion imaging at 193 nm.[1]

Enhancement of optical resolution in immersion media with respect to air is described by Rayleigh's criteria, $R = \frac{k_1 \lambda}{n \sin\theta} = \frac{k_1 \lambda}{NA}$. It states that the minimum resolvable pitch is inversely proportional to numerical aperture of the objective lens. Imaging in a liquid media makes the numerical aperture larger than 1, which is the upper limit for imaging in air. Equivalently, it can be argued that the light has a shorter wavelength in liquid. In addition to resolution enhancement, immersion lithography also results in a larger depth of focus, $DOF = \pm \frac{k_2 n \lambda}{NA^2}$. A numerical aperture larger than 1 can be achieved by immersing the whole wafer in an immersion media. However, the high volume nature of microelectronics manufacturing and its stringent environment requirements makes the idea of total immersion too awkward to be put into a production line. Alternatively, an introduction of a thin immersion liquid between the wafer and the final lens can create an equivalent enhancement of numerical aperture. This is the most practical and widely adopted optics configuration. Among the candidates for immersion liquids, water appears to be an excellent choice due to its high transmission at a wavelength of 193 nm, as well as immediate availability and low processing cost. However, air bubbles are often generated in the process of introducing a water fluid layer between the resist and lens surfaces due to the high surface tension of water. The presence of air bubbles not only causes scattering of exposure light but also poses risks of forming defects that are the images of the bubbles themselves if they are close or attached to the surface of the wafer, i.e. the imaging plane. In Owa[3], the formation, prevention and elimination of bubbles was discussed. According to this paper, bubble formation occurs when the gas-saturated water is shifted to a state of over-saturation due to changes in external conditions, *i.e.*, pressure, temperature. The mechanism suggests that degassing is an efficient way to prevent bubble formation. In spite of the plausibility of preventing bubble formation via degassing, it is still essential to understand the effect the presence of air bubbles has on image quality since complete suppression of air bubbles seems difficult.

2. GEOMETRICAL OPTICS MODEL OF BUBBLE SCATTERING

Scattering of air bubbles in water can be approximately described using a geometrical optics model.[4] An air bubble assumes a spherical shape in water when the hydraulic pressure due to gravity is ignored. The assumption is reasonable in lieu of immersion lithography where a thin layer of water with thickness of about 0.5 mm is applied. The reflection/refraction at the spherical interface causes the to light stray into various directions, i.e. scattering. The relevant reflection/transmission coefficients can be approximated by flat surface Fresnel coefficients. However, the air bubble in water is a special case, where the refractive index of the bubble is less than that of the surrounding media, resulting in a contribution of total reflection to scattered irradiance at certain angles. The situation is described in Fig. 1. For an arbitrary ray incident on a bubble, the angle of incidence is $i = arcsin(s/a)$, where a is the radius of the bubble, s is the deviation from the center. The critical incident angle is

$$i_c = arcsin(n_i / n_w) \quad \textbf{(1)}$$

where n_i is the refractive index of the air, n_w is the refractive index of water. The corresponding critical scattering angle is

$$\theta_c = 180° - 2i_c \quad \textbf{(2)}$$

At a wavelength of 193 nm, the refractive index of water is n_w=1.437. Therefore, the critical incident angle and critical scattering angle are,

$$i_c = arcsin\left(\frac{1}{1.437}\right) = 44°$$

$$\theta_c = 180° - 2i_c = 92°$$

The presence of total reflection greatly enhances the light scattered into the region subtended by $0 \le \theta \le \theta_c$. In this case, the region covers all the forward directions. Hence, air bubbles in water cause strong scattering in all the forward directions. However, a complete understanding of scattering will require taking into account the effects of interference of the reflected light with other transmitted light. The rigorous solution of the scattering pattern can be numerically evaluated by partial wave (Mie) theory. The Mie calculations are discussed in the following section.

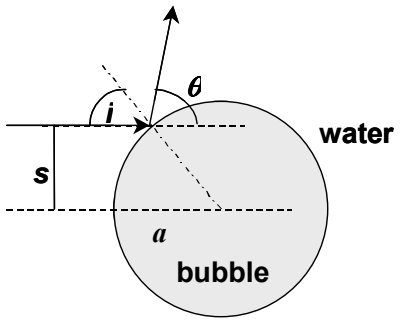

Fig. 1. Reflection of a ray from a spherical bubble in water. Total reflection occurs when the incident angle *i* is larger than the critical angle, $\sin^{-1}[n_i / n_w]$.

3. EXACT COMPUTATION OF SCATTER

In Mie scattering theory,[5] the incident, scattered, and internal fields are expanded in a series of vector spherical harmonics. The coefficients of these expansion functions are chosen so that the tangential components of the electric and magnetic fields are continuous across the surface of the sphere. Two calculation parameters are needed to specify a scattering case, the relative refractive index $m = n_i / n_w$ and the size parameter $ka = 2\pi \frac{n_w a}{n_i \lambda_i}$. The scattering irradiance can be calculated from equation (3) and (4),

$$i_j = i_{inc} I_j a^2 / 4R^2 \quad \textbf{(3)}$$

$$I_j = \left|S_j\right|^2 (2/ka)^2 \quad \textbf{(4)}$$

where subscript *j* denotes the polarization orientation (*j=1*, perpendicular to scattering plane; *j=2*, parallel to scattering plane). The term i_j is the scattered irradiance, i_{inc} is the incident irradiance, I_j is the normalized scattered irradiance, *R* is the distance from the bubble to the far-field observation point, and S_j is the complex scattering amplitudes. S_j can be evaluated from the Mie series.

At the wavelength of 193 nm, the scattering of an air bubble 2 μm in diameter was calculated according to Mie theory and plotted in Fig 2. The refractive index of water at this wavelength is 1.437. The logarithm of relative scattered irradiance was plotted against lateral distance instead of the usual angular direction in the Mie calculation, because this is the situation where the resist film is exposed to the scattered irradiance. The scattered irradiances at distances of 100, 200, 500, 1000 μm from the bubble are plotted in the figure. As shown in the figure, the scattered irradiance dies off quickly and the distribution in the lateral direction becomes more uniform. It indicates that the bubbles further from the resist have less effect on resist imaging.

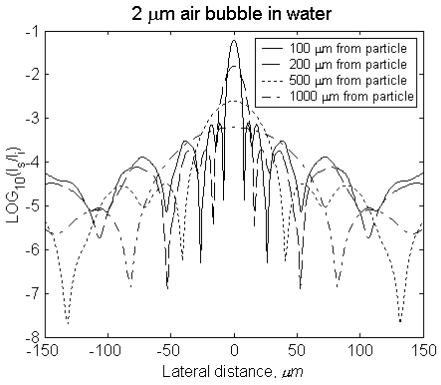

Fig. 2. Lateral distribution of relative scattered irradiance of an air bubble in diameter of 2 μm from various distances from the bubble.

The fact that the bubble size and population in the water cannot be precisely controlled delivers extra difficulties to experimental bubble-scattering studies. Therefore, it would be beneficial to find synthetic spheres that are stable in water and possess similar scattering properties to air bubbles so that they can be used to mimic air bubble scattering in water. At the wavelength of 193 nm, air bubbles are transparent with a refractive index of approximately 1.0. Ideally, a synthetic sphere with refractive index of 1.874+0*i* (so that the refractive index difference with water is the same as air bubble) would serve the purpose. Unfortunately, synthetic spheres with this index were not commercially available. Polystyrene (PST) beads (n=1.67+1.02*i*) and PMMA (n=1.55+0.01*i*) are the closest matches. Mie scattering calculations of Polystyrene and PMMA beads 2 μm in diameter are conducted with the results plotted in Fig. 3 and Fig. 4 respectively. The results suggest that PST beads have a similar scattering pattern to air bubbles even though PMMA is more transparent at 193 nm. The 2-D distribution of scattered irradiance about air bubble, PST and PMMA were plotted in Fig. 4, Fig. 5 and Fig. 6 respectively. It is obvious that the scattering pattern of PST beads resembles that of air bubble, especially in the forward direction. The results further suggest that PST beads are suitable to mimic air bubble in scattering study.

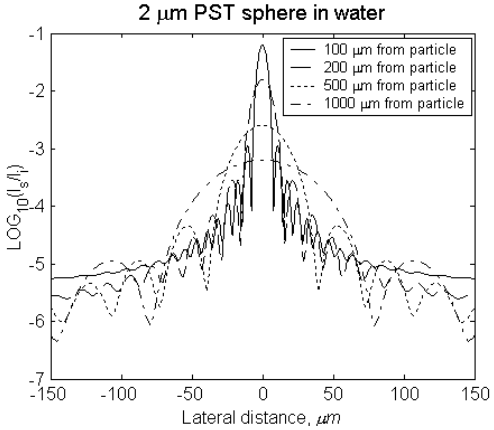

Fig. 3. Lateral distribution of relative scattered irradiance of polystyrene sphere 2 μm in diameter from various distances from the bubble.

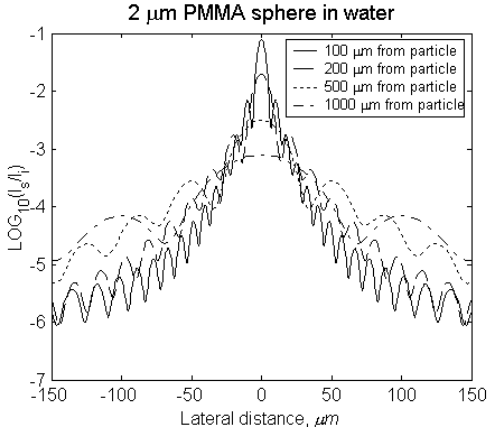

Fig. 4. Lateral distribution of relative scattered irradiance of a PMMA sphere 2 μm in diameter from various distances from the bubble.

The size of the bubble is another important parameter determining its scattering pattern. In Fig. 8 and Fig. 9, the Mie scattering patterns of air bubbles 1 μm and 0.5 μm in diameter were plotted respectively. Along with Fig. 5, it can be seen that the scattered irradiance in the forward directions becomes more uniform as the size becomes smaller. It is fair to say that scattering due to smaller bubbles tends to form uniform background irradiance on the resist.

In the above numerical calculations, only one scattering sphere is involved but multiple spheres take part in scattering in a real situation. Due to the random distribution of scattering spheres in the media, the contribution to scattered irradiance from separate spheres is incoherent. The incoherent summation of scattered irradiance from all spheres is the total scattered irradiance. The Mie scattering calculation of two bubbles 2 μm in diameter with 100 μm separation was plotted in Fig. 10, Fig. 11, and Fig. 12, for unpolarized, TE-polarized, and TM-polarized illumination, respectively. The scattered irradiance on the resist film is averaged to be more like a uniform background due to contributions from multiple spheres.

In a lithographic imaging system, at least two beams are needed to resolve a useful image. That means that an air bubble in the optical path scatters two coherent incident beams. The resulting scattered irradiance is the coherent summation of the single beam scattered irradiance. The Mie scattering patterns of two-beam scattering for an air bubble in diameter of 2 μm were plotted in Fig. 13, Fig. 14 and Fig. 15 for unpolarized, TE-polarized and TM-polarized illumination for the case of numerical aperture equaling 1.2 where the oblique angle in water is 56°.

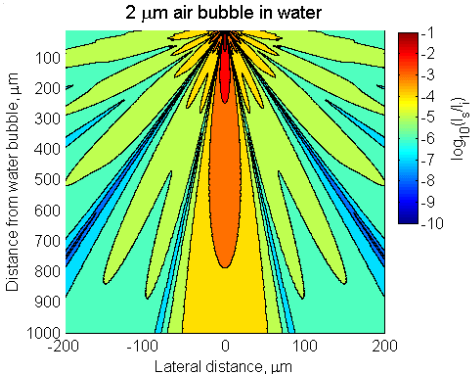

Fig. 5. Distribution of relative scattered irradiance of an air bubble 2 μm in diameter in water.

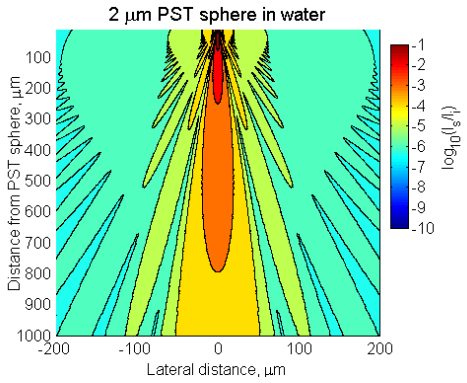

Fig. 6. Distribution of relative scattered irradiance of a polystyrene sphere 2 μm in diameter in water.

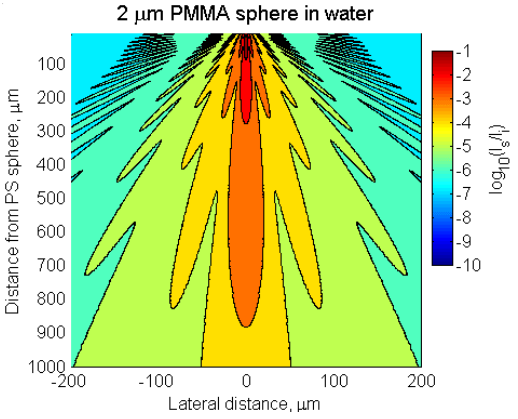

Fig. 7. Distribution of relative scattered irradiance of a PMMA sphere 2 μm in diameter in water.

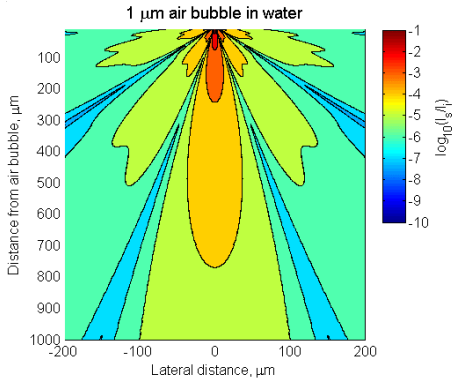

Fig. 8. Distribution of relative scattered irradiance of an air bubble 1 μm in diameter in water.

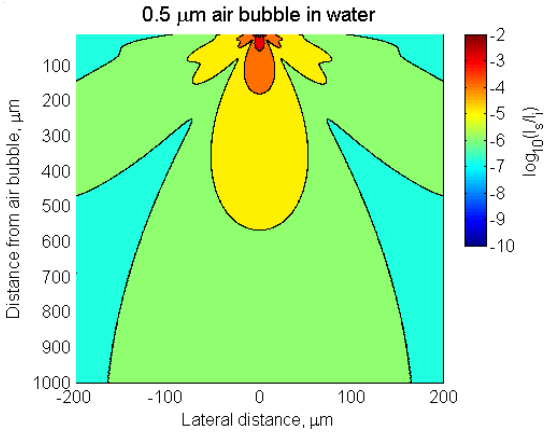

Fig. 9. Distribution of relative scattered irradiance of an air bubble 0.5 μm in diameter in water.

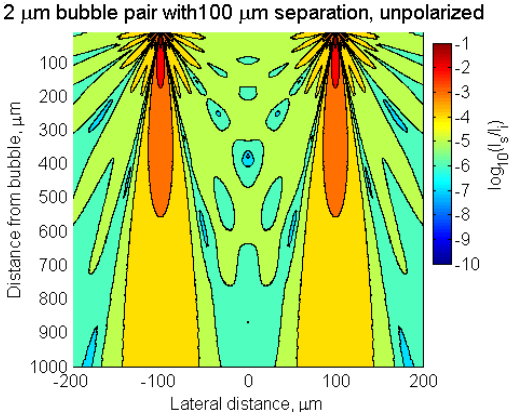

Fig. 10. Distribution of relative scattered irradiance of 2 air bubbles 2 μm in diameter separated by 100 μm in water under unpolarized irradiation.

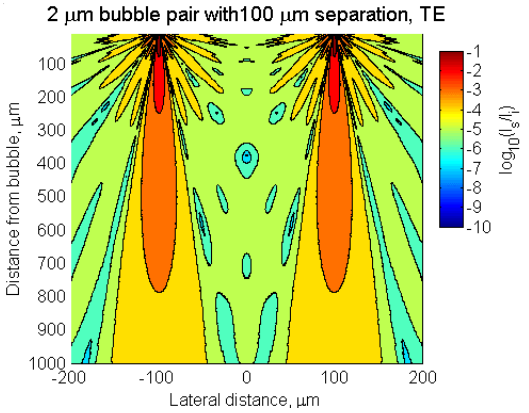

Fig. 11. Distribution of relative scattered irradiance of 2 air bubbles 2 μm in diameter separated by 100 μm in water under TE-polarized irradiation.

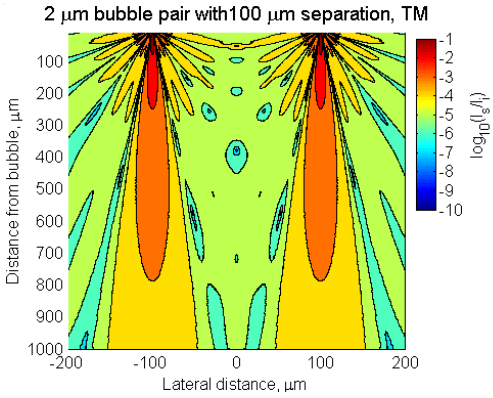

Fig. 12. Distribution of relative scattered irradiance of 2 air bubbles 2 μm in diameter separated by 100 μm in water under TM-polarized irradiation.

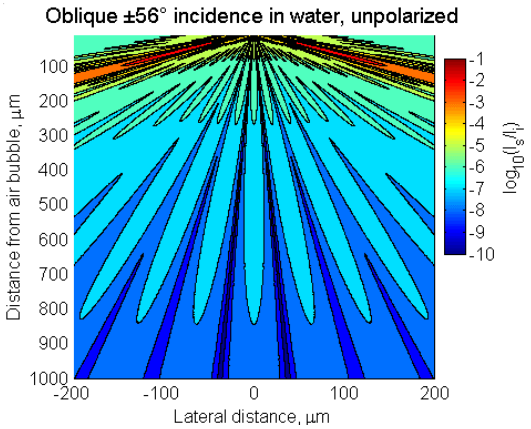

Fig. 13. Distribution of relative scattered irradiance of an air bubble 2 μm in diameter in water illuminated by two oblique (±56º) beams without polarization

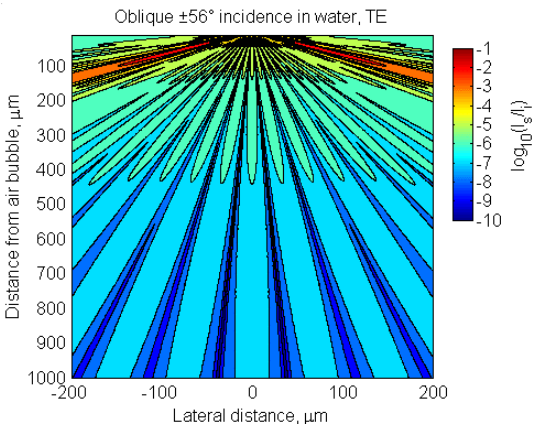

Fig. 14. Distribution of relative scattered irradiance of an air bubble 2 μm in diameter in water illuminated by two oblique (±56º) beams with TE-polarization

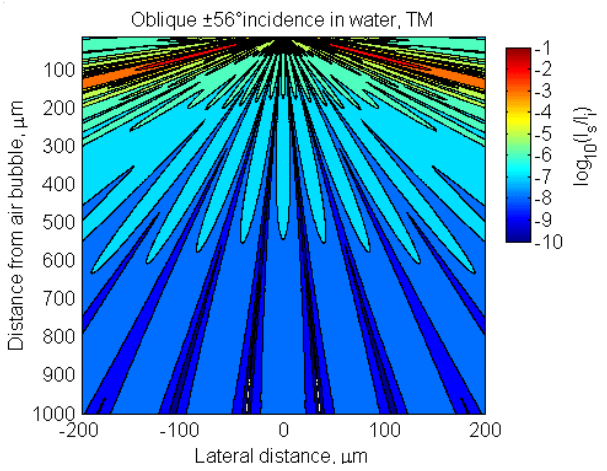

Fig. 15. Distribution of relative scattered irradiance of an air bubble 2 μm in diameter in water illuminated by two oblique (±56º) beams with TM-polarization

4. SCATTERING MEASUREMENTS

A modified UV VASE tool was used to measure Variable Angle Scattering (VASS). The relative scattered irradiance of PST beads (2 μm in diameter, 2×10^{-4} %) at 10º off the forward direction was plotted versus wavelength in Fig. 16. The corresponding Mie scattering calculation was plotted in Fig. 17. The results show that our experimental measurements agree with Mie theory, so we are confident with our numerical calculations.

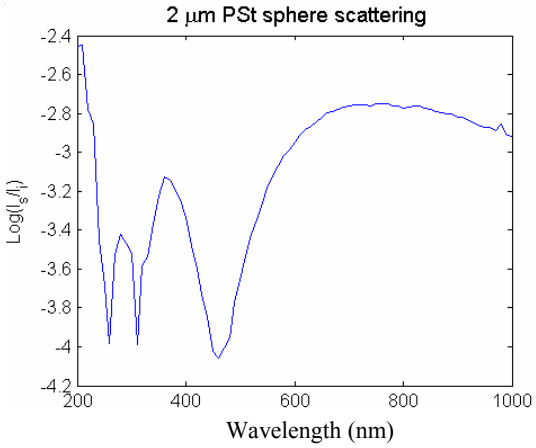

Fig. 16. Measured relative scattered irradiance of PST beads (2 μm in diameter, 2×10^{-4} %) at 10º off the forward direction

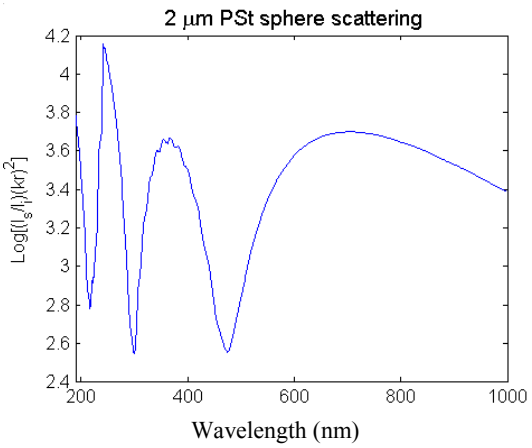

Fig. 17. Mie Scattering calculation for PST beads (2 μm in diameter), at 10º off the forward direction

5. LITHOGRAPHIC IMAGING OF "BUBBLES"

The purpose of this paper is to find a clue to the question "what if there are air bubbles in water gap in immersion lithography?". The presence of air bubbles affect imaging in two ways: 1) scattering of exposure light; 2) causing defects if the bubble are actually imaged on the resist. The first issue can be characterized as "flare" while the second issue has the potential to be a yield killer. It is beneficial to understand under what circumstances the bubbles will actually be printed on the resist. Experimental studies on the imaging actual bubbles would be hard because the size and population of artificially generated air bubbles are not well controlled. Previous numerical calculations of Mie scattering in this work have suggested that PST beads could be used to mimic air bubbles due to their similar scattering patterns to those of air bubbles. In this work, PST beads were suspended in HPLC water which was then used as immersion lithographic media for air bubble scattering study.

The first experimental set-up is shown in Fig. 18. A water gap suspended with PST spheres 2 μm in diameter is formed between a resist-coated wafer and a 0.6 mm fused silica flat plate. The thickness of the water gap is controlled by spacers with thickness larger than Λ^2/λ. A phase grating with 600 nm pitch is placed on top of the flat plate, groove side facing down. The total number of spheres that could be imaged on the resist can be calculated from the sphere concentration and the optical path length, while the total number of spheres that are eventually printed on the resist can be found out by counting the "bubble" images on the resist. The results are plotted in Fig. 19. As shown in the figure, the total number of "bubbles" in the optical path increases proportionally with water gap thickness while the total number of imaged "bubbles" levels off at about 0.3 mm. It indicates that the "bubbles" which are 0.33 mm or farther away from the wafer will not be imaged.

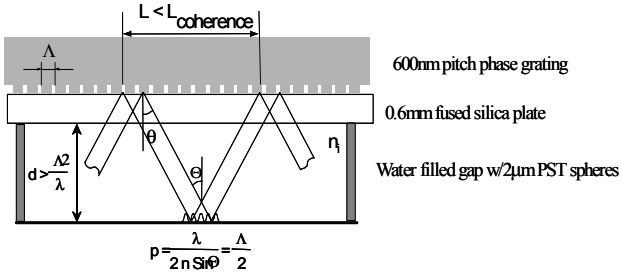

Fig. 18. Set-up for direct lithographic imaging of "bubbles".

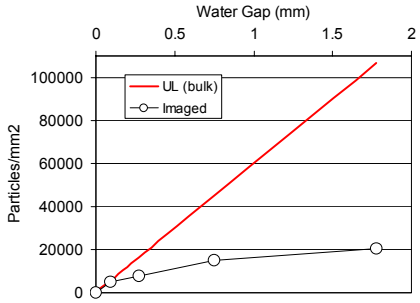

Fig. 19. Total number of "bubbles" in optical path versus total number eventually imaged.

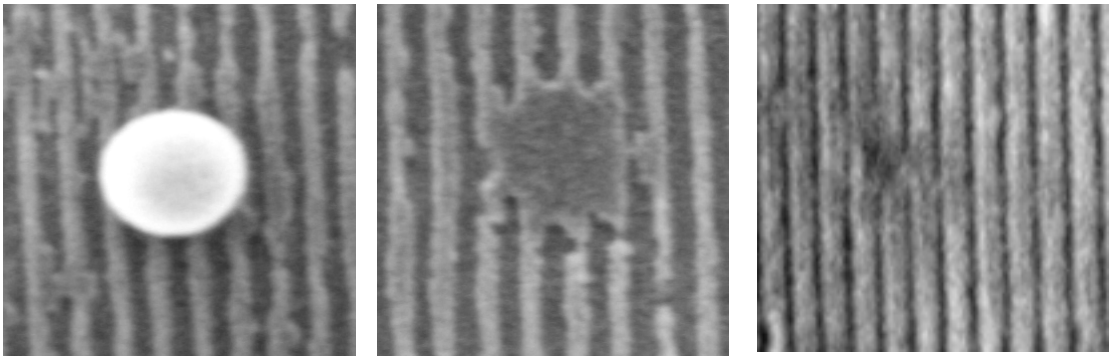

(a) PST sphere; (b) PST sphere image in resist; (c) PST sphere image in resist.

Fig. 20. SEM pictures of a PST sphere and their image in resist.

The second experimental set-up is shown in Fig. 21. As shown in the figure, the laser beam is turned to a phase grating after beam-expanding. The ±1 orders are directed towards the wafer where two-beam interference occurs. The water gap suspended with PST spheres is contained between the wafer and a silica flat plat or half ball. The thickness of the water gap is controlled by spacers. The NA value determines the use of the flat plate or the half ball. A series of experiments were conducted at NA=0.5 with PST spheres 2 μm in diameter were conducted. Following a similar methodology as the first experiment, it is found that the "bubbles" which are 0.33 mm or farther away from the wafer will not be imaged. A SEM picture of the "bubble" and "bubble" image in resist is shown in Fig. 21. The results of polystyrene spheres 0.5 μm in diameter of at $2.5x10^{-5}$ weight concentration are surprising. None of the "bubbles" are actually printed in the resist, as shown in Fig. 22, though the sphere is much larger than the line-width (100 nm). If a PST sphere was in contact with the resist, it would be printed in the resist. It is likely that the surface tension repels the PST spheres away from the resist film to the distance beyond which they will not be printed. It can be argued that this distance for a 0.5 μm PST sphere is very much smaller than 1.3 mm, beyond which PST spheres 2 μm in diameter will not print.

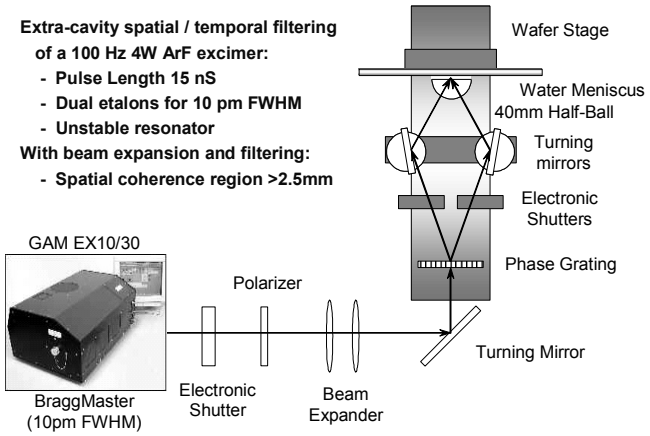

Fig. 21. Interferometric system for "bubble" imaging.

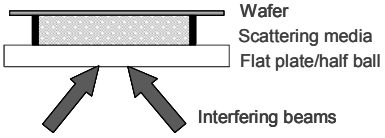

Fig. 22. Set-up for two-beam interference through scattering media

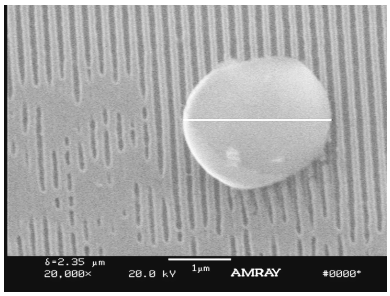

Fig.21. Interferometric image in water suspended with polystyrene beads of 2 μm diameter at $5x10^{-5}$ weight concentration.

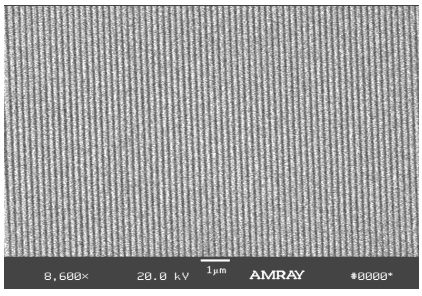

Fig.22. Interferometric image in water suspended with polystyrene beads of 0.5 μm diameter at $2.5x10^{-5}$ weight concentration.

6. CONCLUSIONS

In this work, scattering induced by an air bubble in water was first analyzed by geometrical optics. The total reflection of light causes the enhancement of scattering in the region where the scattering angle is less than critical scattering

angle. At 193 nm, the calculated critical scattering angle is 92 degrees, indicating a strong scattering in all the forward directions. A rigorous scattering solution was numerically evaluated by partial wave (Mie) theory. Mie scattering of air bubbles was compared with that of polystyrene and PMMA spheres at 193 nm in the cases of TE, TM or unpolarized incident light. Multiple particle scattering as well as two oblique beams scattering was also numerically computed. Analysis of the scattering patterns shows that the scattering effects of PST spheres resemble those of air bubbles in water. The Mie results of polystyrene spheres were verified by actual scatterometry measurements on a modified UV VASE tool.

Lithographic imaging of "bubbles" in an immersion water gap was studied by mimicking air bubbles with polystyrene spheres. By counting the number of "bubbles" which are actually imaged and evaluating the number of "bubbles" which are present in the optical path, the distance beyond which "bubbles" will not print can be estimated. In direct interference lithography, this distance is found to be 0.3 mm in the case of PST spheres 2 μm in diameter. In interferometric lithography at 0.5NA, this distance is estimated to be 1.3 mm in the case of PST spheres in diameter of 2 μm. Repelling of "bubbles" from the resist film by surface tension was proposed to explain the fact that PST spheres 0.5 μm in diameter will not image. The conclusion can be drawn that actual imaging of an air bubble in the resist depends on the size of the bubble and its distance from the resist film while scatter of exposure light can be characterized as "flare".

The work reveals that microbubbles are not a technical barrier to immersion lithography. Nevertheless, degassing of immersion water is very necessary. Also, consideration should be taken to minimize the possibilities of trapping air when designing water-introducing devices.

7. REFERENCES

1. B. W. Smith, H. Kan, *et al*, "Water immersion Optical Lithography for the 45 nm node", SPIE Optical Microlithography XVI, pp. 679-689, 2003.
2. B. J. Lin, "The k_3 coefficient in nonparaxial λ/NA scaling equations for resolution, depth of focus, and immersion lithography", JM^3 **1**(1), pp. 7-12, 2002.
3. S. Owa, H. Nagasaka, "Immersion lithography: its potential performance and issues", SPIE Optical Microlithography XVI, pp. 724-732, 2004.
4. P. L. Marston, "Light scattering from bubbles in water", Ocean 89 Part 4 Acoust Arct Stud, pp. 1186-1193, 1989.
5. C. F. Bohren, D. R. Huffman, *Absorption and Scattering of Light by Small Particles*, John Wiley & Sons, 1983